Turkish Journal of Chemistry

http://journals.tubitak.gov.tr/chem/

Research Article

Turk J Chem
(2014) 38: 1135 – 1152

doi:10.3906/kim-1407-15

Synthesis and properties of novel polymeric metal-free and metallophthalocyanines containing peripherally long 1,2-bis[(3-oxapropyl)oxa]benzene derivatives

Ahmet BİLGİN[1,*], **Durmuş YANMAZ**[2], **Çiğdem YAĞCI**[1]
[1]Department of Science Education, Kocaeli University, Kocaeli, Turkey
[2]Department of Science Education, Muğla Sıtkı Koçman University, Kötekli, Muğla, Turkey

Received: 05.07.2014 • **Accepted:** 03.09.2014 • **Published Online:** 24.11.2014 • **Printed:** 22.12.2014

Abstract: New polymeric phthalocyanine moieties (M = 2H, Zn, Ni, Cu, and Co) were synthesized via polytetracyclomerization reaction of *o*-bis[3-(3,4-dicyanophenoxy)propyloxy]benzene (**3**), which can be obtained by the reaction of 4-nitrophthalonitrile with *o*-bis[(3-hydroxypropyl)oxy]benzene. Aggregation and disaggregation behavior of the polymeric phthalocyanine (**5**) was studied with some alkali and earth alkali metal cations. Measured intrinsic viscosities of the polymeric phthalocyanines exhibited a substantial decreasing tendency with dilution of the solution. Thermogravimetric analysis was performed under air by using DSC and DTG/TGA techniques and indicated that these polymers have good thermal stability. AC and DC electrical conductivities of the polymeric phthalocyanines were investigated in the frequency range 100 Hz–1 MHz within the temperature range 298–343 K. AC/DC conductivities of the samples were found to be between 10^{-5} and 10^{-7} S cm^{-1} at ambient temperature under argon atmosphere. The structures of new synthesized compounds were characterized by using microanalysis; various spectroscopic methods such as UV-Vis, FT-IR, ^{1}H NMR, and ^{13}C NMR spectroscopy; and MS spectra.

Key words: Polymeric phthalocyanine, metallophthalocyanines, aggregation, AC/DC electrical conductivities, thermal properties, DSC/TGA

1. Introduction

Low-molecular weight phthalocyanines[1,2] and their polymeric derivatives[3,4] are attracting great attention because of their high thermal and chemical stability,[5] high gas sensitivity,[6,7] excellent semiconducting behavior,[1,2,6,7] and biological importance due to their similar molecular structure to metalloporphyrins.[1,2,8] The attention to the usage of phthalocyanines is increasing in many fields such as dyestuffs,[9] electric conductors,[10] catalysts,[1,2] electrocatalysts,[3,4,11] electrochemically active layers,[12] cathode materials in Li-batteries,[13] photovoltaic or photogalvanic elements,[14] and sensitizers for photodynamic therapy of cancer (PDT).[15,16]

Metal-free and metallophthalocyanines containing single phthalocyanine cores are mostly prepared via cyclotetramerization reaction of phthalic acid derivatives, such as *o*-benzonitrile or phthalic anhydride derivatives or 1,3-diminiisoindoline derivatives, under different reaction conditions in the absence or presence of metals or metal salts, in high yields.[17] However, polymeric phthalocyanines bearing multiple phthalocyanine cores can be synthesized via polycyclotetramerization under appropriate reaction conditions using bifunctional monomers

*Correspondence: abilgin@kocaeli.edu.tr

as precursor, like 1,2,4,5-benzenetetracarbonitrile and other various sulfur, arylenedioxy-, alkylenedioxy-, and oxy-bridged diphthalonitrile derivatives and other nitriles or tetracarboxylic acid derivatives.[18–20] The polymeric phthalocyanines were found to have higher conductivity, better catalytic properties, and better thermal stability than monomeric phthalocyanine analogues.[21–24] Furthermore, they possess large and accessible surface areas and are of great technological importance for adsorption and heterogeneous catalysis.[25] The insolubility of polymeric phthalocyanines in water and common organic solvents restricts their usage in some fields and makes their structural investigations difficult.[24]

We have previously presented several types of peripherally tetra- and octa-substituted hydroxyl-functionalized monomeric phthalocyanines[26,27] and peripherally mixed nitrogen- and oxygen-donor moieties,[28] only sulfur linkage moieties,[29] and lariat ether[30] substituted polymeric phthalocyanines.

In this article, the preparation and properties of new polymeric phthalocyanines bearing peripherally 1,2-bis[(3-oxapropyl)oxa]benzene derivatives is described. Using a bisphthalonitrile fused flexible unit is an advantage for the preparation of polymeric phthalocyanines with high molecular weight.[29,31] The AC and DC electrical conductivity of the polymeric phthalocyanines was measured by using a sandwich form cell in argon atmosphere. The intrinsic viscosity behaviors of the prepared polymers were examined at ambient temperature. The visible electronic spectra of compounds **4**–**8** were investigated in pyridine with different concentrations. Aggregation or disaggregation properties of polymer **5** with some alkali and earth alkali metals were also studied. Thermoanalytic techniques such as DSC and DTG/TGA were used to investigate the thermal properties of compounds **3**–**8**. The structures of the novel compounds were identified with microanalysis, UV-Vis, FT-IR, NMR, and MS spectral data.

2. Results and discussion

2.1. Synthesis and characterization

o-Bis[(3-hydroxypropyl)oxy]benzene (**1**) was synthesized according to the literature[32,33] by the reaction of catechol and 3-chloro-1-propanol in EtOH, by modifying the relevant procedures (Scheme). The yield (81%) of **1** was higher than that obtained by the known procedures (60% or 65%).[32,33] The mass spectral data of **1** showed a peak of m/z = 251.2274 corresponding to $[M + Na + 2]^+$. The microanalysis of **1** was in accordance with the theoretical calculation. The ^{1}H NMR spectrum of **1** in $CDCl_3$ shows signals at δ = 6.86–6.82 (m, 4H, Ar*H*), 4.11 (t, J = 5.7 Hz, 4H, ArOC*H*$_2$), 3.80 (t, br, J = 5.0 Hz, 4H, $OCH_2CH_2CH_2OH$), 1.99 (p, J = 5.9 Hz, 4H, $OCH_2CH_2CH_2OH$), and 1.68 (s, br, 2H, OH) ppm. Furthermore, the signal at 1.68 ppm related to the protons of O–H groups was replaced with deuterium with the treatment of D_2O, and a new signal appeared resulting from HOD at 4.67 ppm. In the ^{13}C NMR spectrum, compound **1** exhibits the primary alcohol carbon atoms at δ= 61.13 ppm (CH_2OH) and the other aromatic and aliphatic carbon atoms were observed at 148.34 (Ar*C*O), 121.32 (Ar*C*H), 112.97 (Ar*C*H), 67.80 (ArO*C*H$_2$), and 31.73 ($OCH_2CH_2CH_2OH$) ppm, respectively. In the IR spectrum of **1**, both O–H and H–O$\cdots$H stretching vibrations appeared at 3400 and 3342 cm^{-1}, respectively.

o-Bis[3-(3,4-dicyanophenoxy)propyloxy]benzene (**3**) was prepared by the nucleophilic aromatic substitution reaction[34–36] of 4-nitrophthalonitrile with compound **1** in the presence of dry K_2CO_3 as a base catalyst and dry DMF. The ESI$^+$ mass spectrum of **3** showed the molecular adduct of Na and K in addition to the M + 1 peak. In the ^{1}H NMR spectrum of **3**, the OH protons observed at 1.68 ppm in compound **1** disappeared and new signals related to aromatic bisphthalonitriles appeared. Additionally, the other protons signals of **3** were

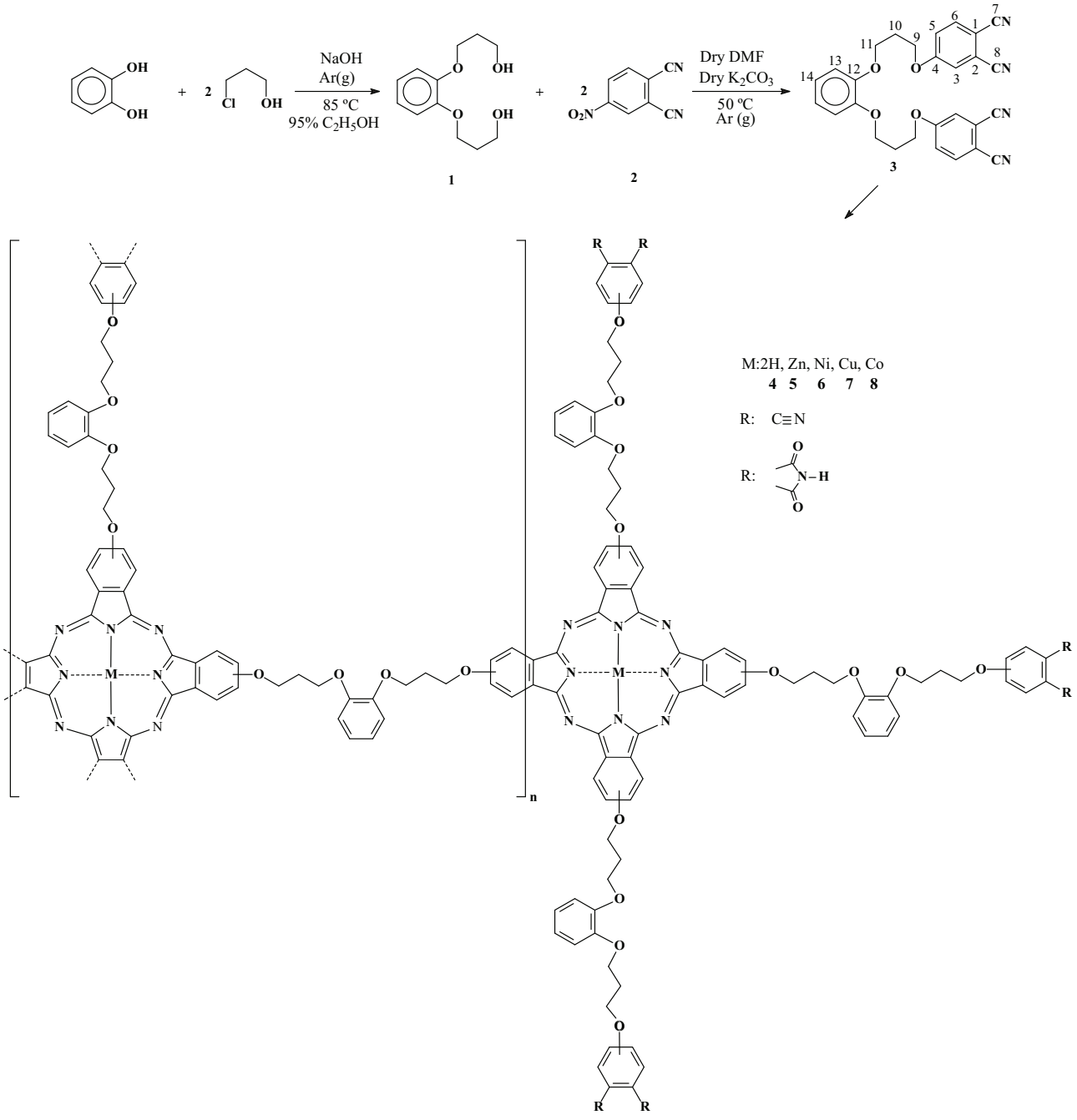

Scheme. Synthesis of the bisphthalonitrile **3** and compounds **4**, **5**, **6**, **7**, and **8**.

slightly shifted except for the signal belonging to $(NC)_2ArOCH_2$. The nitrile carbon atoms (C_7, C_8) of the compound appeared at 116.25–115.60 ppm in the ^{13}C NMR spectrum of **3**. The presence of the C≡N group at 2227 cm^{-1} in the IR spectrum of **3** supported the proposed structure. The obtained microanalysis data for **3** are in compliance with the calculated data.

Compound **4**, $(H_2Pc)_n$, was synthesized with a mixture of **3**, DBU, as base catalyst and amyl alcohol at 160 °C under inert conditions. In order to analyze the polymerization degree, model compound **4a** was

prepared by the conversion of the nitrile end groups of **4** to the imido end groups using a minimal amount of 40% H_2SO_4 in a short time due to degradation of the metal-free polymer. When the IR spectrum of **4a** was compared with that of **4**, the peak at 2227 cm^{-1} corresponding to the C≡N groups of **4** had disappeared and new peaks at ∼1770–1716 cm^{-1} and at 3396 cm^{-1} corresponding to the carbonyl and imide groups had appeared, respectively. These findings support the transformation of the cyano groups into imido groups. The inner core N–H stretching and pyrrole ring vibration bands, which are typical for metal-free phthalocyanines, were also observed at 3285 and 1045 cm^{-1} for **4** and 3278 and 1040 cm^{-1} for **4a**.[37,38] Weak absorptions for –C=N– at 1645 cm^{-1} for **4** and at 1652 cm^{-1} for **4a** were also detected. Microanalyses for **4** and **4a** were satisfactory.

Synthesis of metal containing phthalocyanine derivates (**5**–**8**) was described in the Experimental section. Co-containing polymeric phthalocyanine was prepared in both the presence and absence of catalyst and the yield of **8** (84%) in the presence of catalyst was significantly higher than that in the absence of catalyst (49%). The IR spectra of **5**–**8** were similar with small differences. The imido carbonyl groups caused by the presence of water during the synthesis were observed at ∼1771–1705 cm^{-1}. On the other hand, the IR spectrum of **4** was different because of the inner core N–H vibrations.[38] In the IR spectrum of **4**, the cyano end groups were observed at 2224 cm^{-1}. Furthermore, there was a small shift to lower wavelength in many of the IR bands of the metal-free phthalocyanine with respect to the metal analogues.[20,29,39,40] In the FT-IR spectra of the complexes, ligand stretching vibrations independent from the metal and metal–N stretching vibrations could not be observed in the region of 400–100 cm^{-1}. This can be attributed to the recording of the IR spectra of the samples in KBr pellet forms, which have vibrations in the same region.[41]

Various methods are used to determine the polymerization degree of polymers. Here, as used in a few cases,[42] polymerization degree of the polymeric phthalocyanines was determined by the comparison method of IR absorption of end groups with those of suitable bridging groups due to the difficulty in solubility of the polymeric phthalocyanine. For this purpose, the ratio of absorption intensities of the Ar–O–CH_2 etheric groups at around 1225 cm^{-1} to the absorption intensities of the asymmetric C=O groups of the imides at around 1713 cm^{-1} was calculated [compound/$\log_{10} I_{1225}/I_{1713}$: **4a**/1.07, **5**/1.66, **6**/2.03, **7**/1.63, **8**/1.11]. The polymerization degrees follow the order: **6** > **5** > **7** > **8** > **4a**.

Typical UV-Vis absorption spectra were obtained for the polymeric phthalocyanines (**4**–**8**) in pyridine and conc. H_2SO_4 (Table 1). At the slightly lower wavelengths (Table 1), a shoulder corresponding to aggregated or nonaggregated species in conc. H_2SO_4 and pyridine appeared for the polymeric phthalocyanines (**4**–**8**). The UV-Vis spectrum of the metal-free phthalocyanine (**4**) was taken in 25% H_2SO_4 instead of conc. H_2SO_4 because of the slow decomposition caused by hydrolysis in conc. H_2SO_4, which can be seen in Figure 1 as a diminished absorption coefficient at longer wavelengths. On the other hand, the polymeric metal phthalocyanines (**5**–**8**) were stable. When H_2SO_4 was used instead of pyridine, both a significant bathochromic shift and a decrease in absorption intensity were observed. This can be attributed to degradation and weak protonation of the meso nitrogen atoms at the inner phthalocyanine core.

The UV-Vis spectra of **4** are shown in Figure 1. The characteristic split Q-bands due to $\pi \rightarrow \pi^*$ transition of this fully conjugated 18-π electron system[27,43,44] for the metal-free phthalocyanine (**4**) were observed at λ_{max} = 709 and 677 nm with shoulders at 642 and 613 nm in pyridine, which indicates the nonaggregated species. It is known that the nonaggregated metal-free phthalocyanines with D_{2h} symmetry exhibit 2 intense absorption bands at about 700 nm.[45–48] For compound **4**, the main Q band was broadened and shifted to the higher

energy region about 261 nm in a solution of 25% H_2SO_4. The ratio of the intensities of the UV (Soret band transition) to the Vis (Q-band transition) spectra was calculated and found to be $I_{UV}/I_{Vis} \leq 1$ (Table 1). This result means that the structures of **4**–**8** were homogeneous and no poly(isoindoline) co-units appeared during the synthesis.

Table 1. Wavelength and absorption coefficients of the UV-Vis spectra of the polymers.

Compound	M	Solvent	λ(nm)/log (ε)	Ratio[a] UV-Vis
4	2H	Pyridine	709 (2.72), 676 (2.71), 642[c] (2.44), 613 (2.31), 398 (2.43), 328 (3.11), 307 (2.52)	0.93
		25% H_2SO_4[b]	970 (3.08), 840[c] (2.02), 742 (2.05), 373 (1.90), 310 (2.05), 278 (2.38), 248 (2.68)	0.87
5	Zn	Pyridine	687 (3.57), 617[c] (3.02), 348 (3.61), 319 (3.67)	1.03
		H_2SO_4	853 (3.98), 747[c] (3.44), 376 (3.09), 312 (4.11), 250 (3.81)	0.96
6	Ni	Pyridine	680 (2.61), 613[c] (2.22), 386 (2.42), 333 (2.63), 308 (2.20)	0.84
		H_2SO_4	830 (4.10), 736[c] (3.67), 423 (3.57), 306 (4.04), 243 (4.15)	1.01
7	Cu	Pyridine	686 (3.37), 616[c] (3.00), 336 (3.57), 310 (2.82)	0.84
		H_2SO_4	863 (4.06), 759[c] (3.53), 427 (3.50), 380 (3.60), 305 (3.90), 243 (4.15), 218 (4.11)	1.01
8	Co	Pyridine	665 (3.17), 599[c] (2.81), 334 (3.23), 309 (2.64)	0.83
		H_2SO_4	826 (3.84), 738[c] (3.58), 415 (3.39), 297 (4.07), 238 (4.05)	1.05

[a] Intensity ratio of absorption B bands at $\lambda = 218$–319 nm and Q bands at $\lambda = 665$–970 nm ($C = 2 \times 10^{-4}$ g/L in conc. H_2SO_4 and 2×10^{-4} g/L in pyridine). [b] $C = 1.25 \times 10^{-4}$ g/L in 25% H_2SO_4 for **4**. [c] Shoulder.

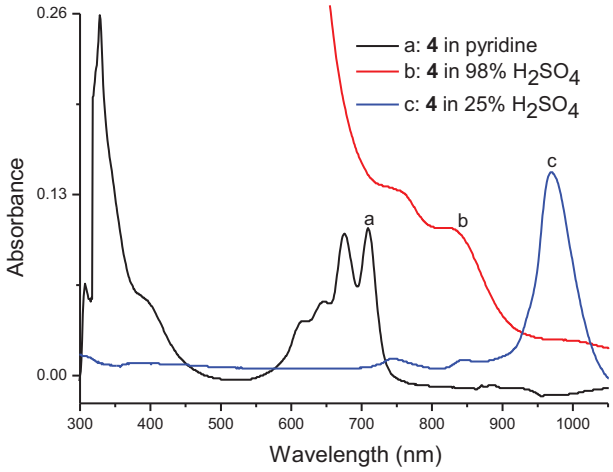

Figure 1. UV-Vis spectra of **4** in pyridine ($C = 2 \times 10^{-4}$ g/L), in 98% H_2SO_4 ($C = 1.25 \times 10^{-4}$ g/L), and in 25% H_2SO_4 ($C = 1.25 \times 10^{-4}$ g/L).

Aggregation can be explained as an overlapped stacking of phthalocyanine units by intermolecular interactions to form dimeric and oligomeric species from monomeric ones. It depends on factors such as polarity of solvent, temperature, concentration of solution, central metal ions, and the nature and position of the substituents.[49–51] The concentration dependent aggregation behavior of **4**–**8** in pyridine was investigated using UV-Vis spectroscopy (Figures 2a–2e and 3a–3e). When the concentration of **5**–**8** was increased, no new bands and no shift of the Q band were observed (Figure 2a–2d).[51] Therefore, we could not determine from Figures

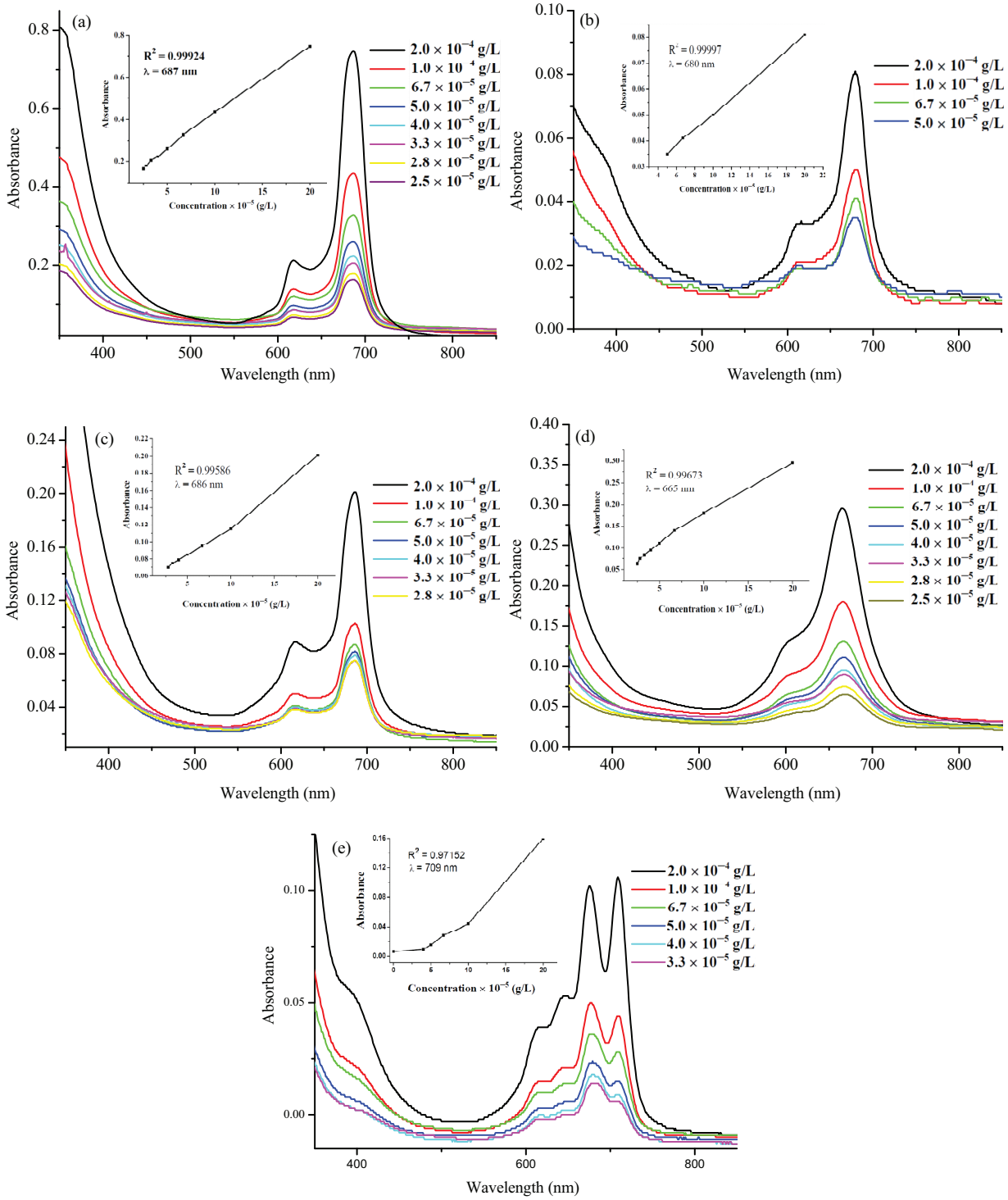

Figure 2. Absorption spectra of **5** (a), **6** (b), **7** (c), **8** (d), and **4** (e) in pyridine at different concentrations. (Inset: Plot of absorbance versus concentration at 687, 679, 686, 665, and 709 nm for compounds **5**, **6**, **7**, **8**, and **4**, respectively).

2a–2d whether there was an aggregation or not. For this reason, $A/\ell C$ versus wavelength was plotted for **5**–**8** and is given in Figures 3a–3d (where A: optical density, ℓ: optical path length, and C: concentration, g/L).

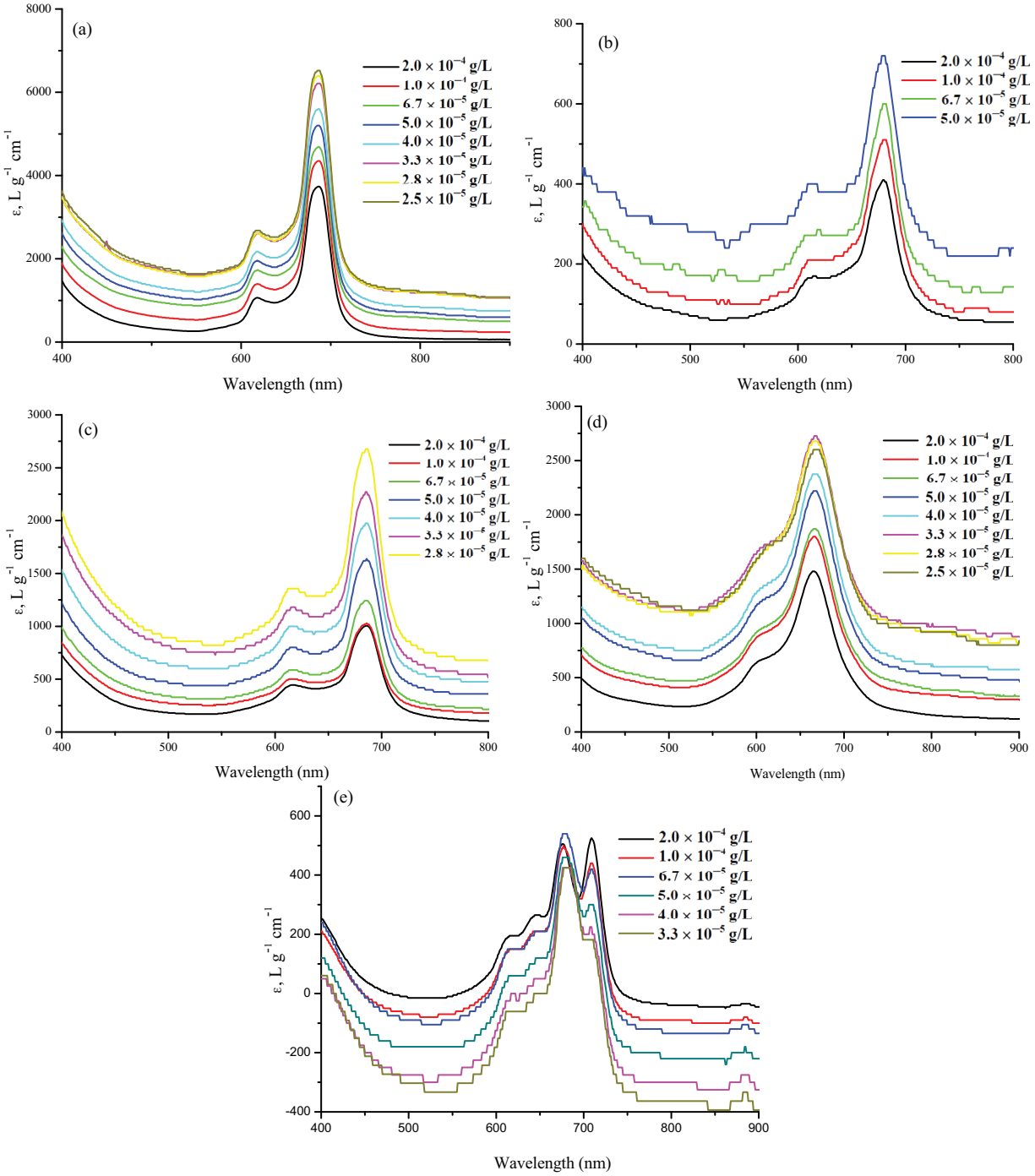

Figure 3. A/ℓC vs. wavelength spectra of **5** (a), **6** (b), **7** (c), **8** (d), and **4** (e) in pyridine at different concentrations.

The extinction coefficients and the intensities of the Q-bands were different as a consequence of aggregation with the increased concentrations of **5**–**8**.[49–51] When the UV-Vis spectra of **4** were examined, the increases in the Q-band intensities were not in the same ratio (Figure 2e). The intensity of the band at 676 nm was higher than that of the band at 709 nm up from 3.3 × 10^{-5} g/L to 1.0 × 10^{-4} g/L concentration range.[29,49] This may be due to the presence of deprotonation of the metal-free phthalocyanine from $(H_2Pc)_n$ to $(HPc)_n^-$

and/or $(Pc)_n^{2-}$ with increasing concentration of pyridine, which can be explained by the transformation of D_{2h} symmetry to D_{4h} symmetry (Figure 2e).[52] Maximum extinction coefficients belonging to the monomer Q-band absorptions are significantly increased with the increasing concentration of **4** (Figure 3e). Figure 3e shows a broader absorbance at the concentrations corresponding to the large decrease in monomer extinction coefficient at 709 nm, indicating the appearance of species with overlapping.[53] Absorbance versus concentration graphs were examined to determine whether compounds **4**–**8** obey the Lambert–Beer law or not (Figures 2a–2e). In Figure 2e, a deviation from the Lambert–Beer law for **4** was observed at the studied concentrations due to the deprotonation of **4** at high pyridine concentrations. The metallophthalocyanines compounds (**5**, **6**, **8**) are nearly compliant with the Lambert–Beer law at the given concentration range. However, the copper phthalocyanine (**7**) obeys the Lambert–Beer law, except at concentrations higher than 1.0×10^{-4} g/L.

The aggregation and disaggregation properties of **5** in pyridine (6.7×10^{-2} g/L) were studied by means of the changes in the visible spectra after the addition of metal salts such as LiCl, $NaNO_3$, KNO_3, $MgSO_4$, $CaCl_2$, $Sr(NO_3)_2$, and $Ba(NO_3)_2$ at different concentrations in methanol. First of all, the effect of increasing methanol concentration on the visible spectrum of **5** in pyridine was examined and no significant differences were observed except for the dilution effect. Then, when Na^+, Li^+, Sr^{2+}, and Ba^{2+} solutions in methanol were added, there was a slight fall in the intensities of the Q absorption bands at 687 and 618 nm without any shift and no optical change. This observation can be ascribed to the weak or no interaction of the peripheral O atoms to Na^+, Li^+, Sr^{2+}, or Ba^{2+} ion in addition to the dilution effect. Despite the diminishing effect of methanol on the intensities of the Q absorption bands, a dramatic change in the visible spectrum of **5** owing to disaggregation was observed when Ca^{2+} solutions in methanol were added. Furthermore, the intensity of the main Q-band of **5** was slightly shifted from 685 to 687 nm. On the other hand, in the case of K^+ and Mg^{2+} addition, confusing changes were obtained in the UV-Vis spectra of **5**. When K^+ solutions in methanol were added, there was an increase in Q-band absorption until 0.2 mL due to the disaggregation of **5**. However, the intensity of the Q-bands was significantly reduced after this concentration. Unlike K^+ addition, a decrease in the intensity of the Q-band until 0.1 mL for Mg^{2+} addition was found. After this concentration, the intensity of the Q-band was increased due to disaggregation.

The measured intrinsic viscosities of freshly prepared solutions of **4**–**8** in conc. H_2SO_4 were similar. The η_{sp}/C values against polymer concentration graphs were plotted and extrapolated to zero concentration to find out the intrinsic viscosities. The viscosities of all polymeric phthalocyanine (**4**–**8**) showed an almost linear reduction with increasing solvent concentrations. This observation may be explained by the decomposition of polymers and weakly protonation of the meso nitrogen atoms in the core of each phthalocyanine unit.

2.2. DSC and DTG/TGA measurements

Thermal properties of **3**–**8** were investigated by DSC (Figures 4 and 5) and TGA/DTG (Figure 6). All the phthalocyanines (**4**–**8**) exhibited both endothermic and exothermic DSC thermograms in the studied temperature range.[45] Broad endothermic peaks in DSC thermograms between 50 and 100 °C are ascribed to the alcohol and water desorption during the synthesis or the adsorbed humidity or air gases' desorption during storage of the samples.[28,54] While compounds **3** and **4** exhibit melting points at 115 and 330 °C (Figure 4), respectively, no melting point is observed for the metallophthalocyanine polymers (**5**–**8**). The main degradation step is visible between 350 and 450 °C with about 22%–84% weight loss for all samples (**3**–**8**) in the TGA/DTG measurements. The initial decomposition temperature is reduced in the order of **4** > **8** > **5**

> **6** > **7** > **3** (Table 2). The most rapidly degraded metallophthalocyanine was Cu-containing polymer (**7**) within the studied polymeric phthalocyanines. However, the other phthalocyanine polymers had good thermal stabilities under air atmosphere and within these temperature ranges.

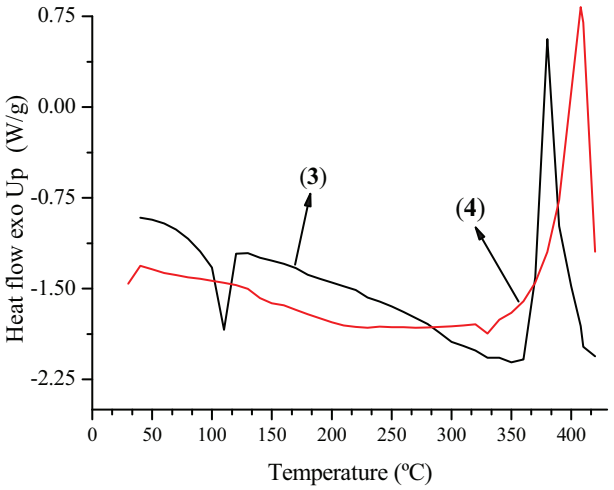

Figure 4. DSC thermograms of **3** and **4**.

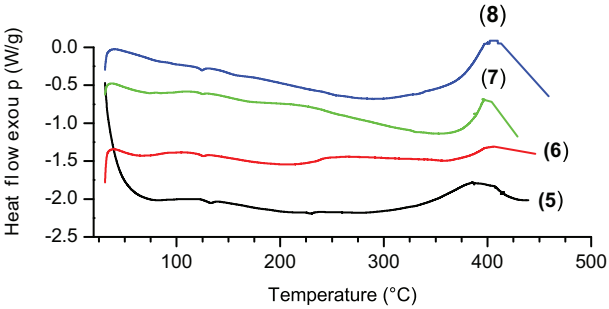

Figure 5. DSC thermograms of **5**–**8**.

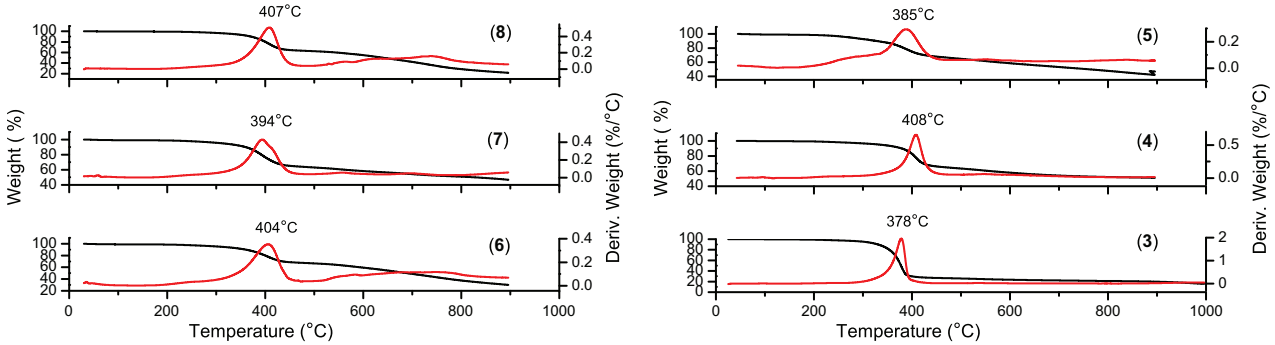

Figure 6. TGA/DTG thermograms of **3**–**8**.

Table 2. Thermal properties of the bisphthalonitrile and its polymeric phthalocyanines.

Compound	Tg (°C)	Melting point (°C)	Initial decomposition temperature (°C)	Main decomposition temperature (°C)
3	–	115	252	378
4	130	330	318	408
5	133	–	300	385
6	124	–	275	404
7	129	–	255	394
8	123	–	306	407

2.3. Conductivity measurements

The AC and DC electrical conductivities of **4**–**8** were determined in argon atmosphere in pellet form 1.3 cm in diameter and 0.10–0.25 cm in thickness coated with aluminum by a vacuum coating system (Univex 300) to form electrodes. The AC and DC conductivity values at different frequencies (1 MHz to 100 Hz) and temperatures

(298 to 343 K) were calculated using the dielectric permittivity and the dielectric loss factor. In order to describe the electrical and dielectric properties of the samples, complex impedance, Z*, measurements were conducted. The relationship between the functions can be given as:

$$Z^* = Z' - jZ'' = 1/(j\omega C_0 \varepsilon^*) \text{ and } \varepsilon^* = \varepsilon' - j\varepsilon'', \quad (1)$$

where $j = \sqrt{-1}$, Z' is the real impedance, Z'' is the imaginary impedance, ε^* is the dielectric permittivity of the sample, ω is the angular frequency of the measured field, and C_o is the capacitance of the empty cell, which is given as

$$C_0 = \varepsilon_0 A/\ell \quad (2)$$

In that, A, ℓ, and ε_0 are active area, distance between the plates, and the vacuum permittivity, respectively. From the real part (Z') the film resistance was found to calculate the AC conductivity of the samples according to the following equation:

$$\sigma = \frac{\ell}{R * A} \quad (3)$$

A typical complex impedance spectrum for compound **7** at 298 K is given in Figure 7. As seen from Figure 7 a single semicircle corresponds to a single relaxation response of the material. This spectrum suggests that in this sample electrode polarization phenomena are absent and the electronic conductivity is predominant.[55]

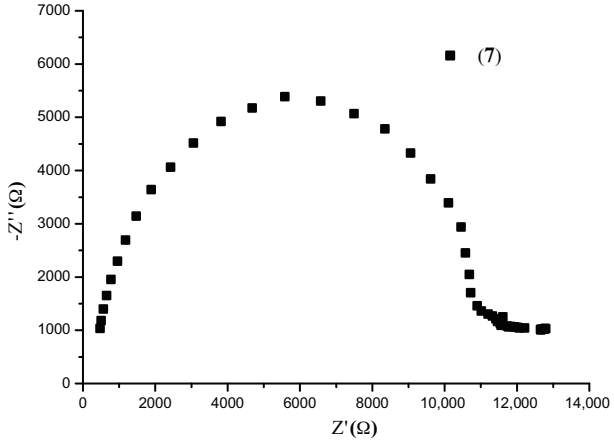

Figure 7. Impedance spectrum of **7** at 298 K.

I-*V* characteristics and DC conductivity of the samples were measured with a Keithley 617 electrometer in argon atmosphere. The electrical conductivities of the samples were calculated according to Eq. (3). The DC conductivity data of **4**–**8** with temperature are plotted in σ versus 1000/T (Figure 8) according to the following Arrhenius equation:

$$\sigma = \sigma_0 \exp(-E_a/2kT), \quad (4)$$

where σ is the specific conductivity, σ_0 is the conductivity as T approaches infinity, E_a is the activation energy, k is the Boltzmann's constant, and T is the absolute temperature. The temperature dependent increase in the DC conductivity may be due to the increase in thermal mobility of the charge carriers and free volume. The thermal activation energy and extrapolated values of compounds are listed in Table 3, which were calculated from the observed slope with the aid of the Eq. (4). Polymeric phthalocyanines were found to have a higher

conductivity than their low molecular weight analogues. This observation may be due to the extension of planarity in the polymer structures that might facilitate greater interaction of the π orbitals of the neighboring phthalocyanine skeletons, thus providing a pathway for charge carriers.[56] The Cu phthalocyanine (**7**), at 298 K, gave the highest σ (3.43×10^{-5} S/cm) and the lowest E_a (0.40 eV). This result may be due to the variations in the intermolecular interactions between polymer chains, which may lead to the increase in conductivity in the Cu phthalocyanine case.[57] The electrical conductivity of the phthalocyanine is generally related to the π electrons of the phthalocyanine core and is owing to thermal excitation of π electrons from the highest filled orbitals to the lowest empty π orbitals. The energy difference between these 2 orbital levels for monomeric phthalocyanine is in the range of 1.5–1.7 eV.[58] The presence of an extended structure in a polymer reduces the band gap, which governs the intrinsic electrical properties.[22] The energy values are much lower in the polymeric phthalocyanines (**4**–**8**) because of the extended conjugated structure (0.40–0.81 eV) as seen in Table 3.

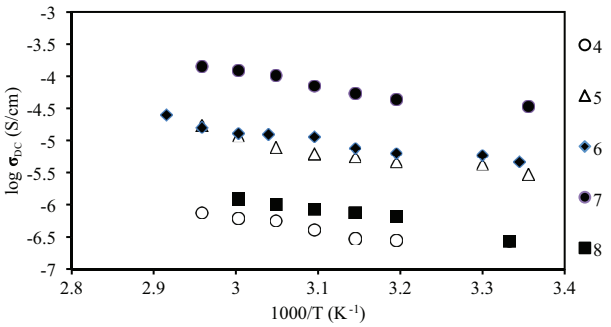

Figure 8. Conductivity versus temperature plot of polymeric phthalocyanines (**4**–**8**).

Table 3. Electrical conductivity and intrinsic viscosities of the polymeric phthalocyanines at room temperature.

Sample no.	σ_{DC} (S/cm)	σ_0 (S/cm)	E_a (eV)	Intrinsic viscosity [η] (H_2SO_4)
4	2.68×10^{-7}	5.27×10^{-3}	0.72	1.62
5	2.97×10^{-6}	0.88	0.71	2.21
6	4.64×10^{-6}	0.58	0.56	2.08
7	3.43×10^{-5}	0.08	0.40	2.20
8	2.72×10^{-7}	0.68	0.81	2.56

The AC conductivity is given by the following equation:

$$\sigma_{AC} = 2\pi\varepsilon_0\varepsilon^* f \tan\delta, \tag{5}$$

where tan δ is the dielectric loss. The loss factor is generally used to characterize the dielectric loss of the materials, which can be defined as the rate of the imaginary part (ε'') to the real part (ε') of the complex dielectric constant,

$$\tan\delta = \varepsilon''/\varepsilon' \tag{6}$$

A plot of AC conductivity as a function of frequency at 298 K is shown in Figure 9. It can be seen from Figure 9 that the AC conductivities of **4**–**8** are nearly independent of the frequency at low frequencies and there is no significant alteration except for **6**. On the other hand, the AC conductivities are strongly dependent on the frequency at frequencies above about 10^4 or 10^5 Hz and there is a clear increase with frequency.[28,59] This is

in good agreement with the theory of AC conduction in amorphous samples suggesting for polaron transport or other hopping modes that the AC conductivity will increase droningly with the increased frequency of the applied field.[60,61]

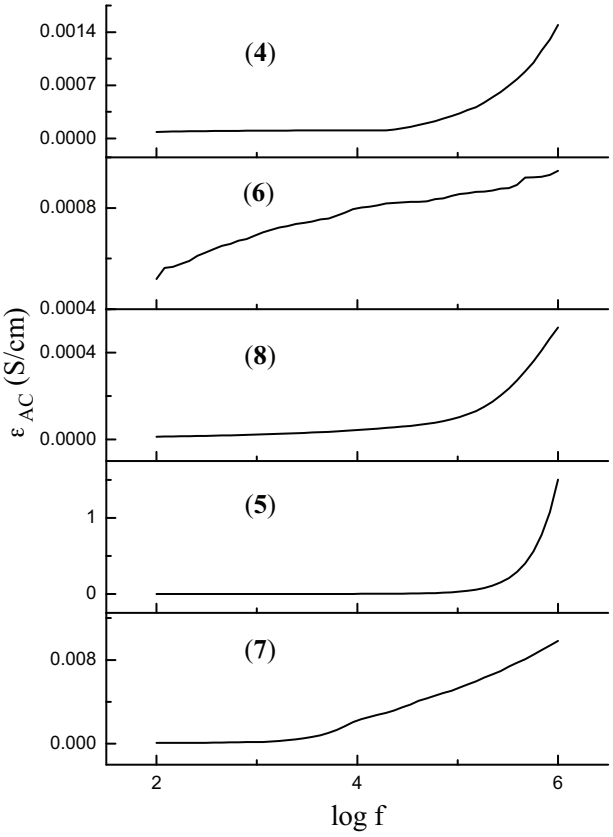

Figure 9. Frequency versus AC conductivity graph at 298 K for polymeric phthalocyanines (**4**–**8**).

In conclusion, the synthesis and characterization of *o*-bis[(3-hydroxypropyl)oxy]-benzene (**1**), *o*-bis[3-(3,4-dicyanophenoxy)propyloxy]benzene (**3**), and the polymeric phthalocyanines **4**–**8** are presented. The polymers (**4**–**8**) were synthesized by the reaction of *o*-bis[3-(3,4-dicyanophenoxy)propyloxy]benzene and the suitable reactants under appropriate conditions. The structures of the new synthesized compounds were characterized by using microanalysis, various spectroscopic methods such as UV-Vis, FT-IR, ^{1}H NMR, ^{13}C NMR spectroscopy, and MS spectral data, and DSC and DTG/TGA techniques. The optical spectra of **4**–**8** in pyridine were obtained at different concentrations. Aggregation tendency was observed for **5** with increasing amounts of methanol, $NaNO_3$, LiCl, $Sr(NO_3)_2$, and $Ba(NO_3)_2$, whereas disaggregation tendency with the addition of $CaCl_2$ was observed. Moreover, the aggregation tendency of **5** showed complex behavior with increasing concentrations of KNO_3 and $MgSO_4$. The intrinsic viscosities of **4**–**8** were found to be between 1.62 and 2.56. The most rapidly degraded metallophthalocyanine was Cu-containing polymer (**7**), whilst the other phthalocyanine polymers had good thermal stabilities under air and within the studied temperature ranges. The electrical conductivity measurements showed that polymeric phthalocyanines are of semiconductor nature. The activation energies of the polymeric phthalocyanines are in the range of 0.40–0.81 eV.

3. Experimental

3.1. Materials

3-Chloro-1-propanol, catechol, 1,8-diazabicyclo[5.4.0]undec-7-ene (DBU), sodium hydroxide (NaOH), phosphorus pentoxide (P_2O_5), hydrochloric acid (HCl), ethanol (EtOH), methanol (MeOH), magnesium sulfate ($MgSO_4$), sodium nitrate ($NaNO_3$), lithium chloride (LiCl), barium nitrate ($Ba(NO_3)_2$), potassium nitrate (KNO_3), strontium nitrate ($Sr(NO_3)_2$), calcium chloride ($CaCl_2$), ammonium molybdate, dimethylsulfoxide (DMSO), chloroform ($CHCl_3$), tetrahydrofuran (THF), dimethylformamide (DMF), pyridine, petroleum ether (PE), *n*-hexane, toluene, amyl alcohol, ethylene glycol, *N*,*N*-dimethylethanolamine (DMEA), acetone, and diethyl ether (Et_2O) were obtained from commercial suppliers. Anhydrous metal salts such as $Zn(CH_3COO)_2$, $NiCl_2$, $CuCl_2$, $CoCl_2$, and K_2CO_3 were used after drying procedures according to the literature.[62–66] 4-Nitrophthalonitrile was synthesized as described in the literature.[34] All the solvents were purified by conventional procedures.[67] All the synthesized products were dried under vacuum over P_2O_5 at 100 °C unless otherwise indicated. The metal analyses of the polymeric metal complexes were conducted as described previously.[28] Metal ion contents in the polymeric metal complexes were determined by atomic absorption measurements after the required processes.

3.2. Techniques

Elemental analysis was carried out using an Elementar Vario MICRO Cube instrument. ^{1}H and ^{13}C NMR spectra were obtained by a Varian UNITY INOVA NMR spectrometer (500 MHz and 125 MHz, respectively) with $CDCl_3$, d_6-DMSO, and D_2O as solvents and tetramethylsilane as an internal standard. Fourier transform infrared (FTIR) spectra were captured on a Shimadzu FTIR-8201 PC spectrophotometer at the spectral range 4000–400 cm^{-1} with samples in KBr pellets. UV-Vis measurements were recorded on a dual beam at ambient temperature on a model T80 + UV-Vis spectrophotometer using quartz cuvettes with a 1-cm path length. An Ubbelohde viscometer was used to measure the intrinsic viscosities of freshly prepared dilute solutions of the polymeric phthalocyanines in conc. H_2SO_4 at room temperature. An Autolab 30 Voltammetry-FRA 2 frequency analyzer and Keithley 617 electrometer were used to record the AC/DC conductivity analysis between 100 Hz and 1 MHz. Mass spectra were obtained on a Bruker Daltonics Microflex mass spectrometer (Bremen, Germany) and a Bruker Daltonics MicroTOF mass spectrometer with orthogonal electrospray ionization (ESI) source. Melting points were determined using an electro thermal digital melting point apparatus (Barnstead Electrothermal IA9100) and are uncorrected. The metal amount in each complex was determined using an atomic absorption spectrophotometer (Unicam 929 AAS). Thermogravimetric experiments (DTG/TGA) were performed using a TA Q500 thermobalance. Materials were scanned at 10 °C min^{-1} and the working temperature range was between 25 and 900 °C. Differential scanning calorimetry (DSC) measurements of samples were performed using a TA Q2000 with a heating rate of 10 °C min^{-1} from 25 to 440 °C.

3.3. Monomer synthesis

3.3.1. *o*-Bis[(3-hydroxypropyl)oxy]benzene (1)

Finely pulverized NaOH (2.80 g, 68 mmol) and 95% EtOH (23.75 mL) were put into a 250-mL 3-necked vessel and mixed at 45 °C for 3 h under argon. After the temperature was reduced to 30 °C, 3-chloro-1-propanol (12 mL, 139.4 mmol) and catechol (3.04 g, 27.4 mmol) were added to the reaction medium. The reaction mixture was stirred for 48 h at 85 °C while the reaction progress was monitored by thin layer chromatography (TLC)

[7:2:1 $CHCl_3$:PE:MeOH]. At the end of the reaction, the cooled reaction mixture was transferred into a beaker. Next 50 mL of EtOH and 10 mL of aqueous solution of NaOH (10%) were added to the beaker content with stirring. The solvent was then evaporated under vacuum using a rotary evaporator. The cooled residue was extracted with Et_2O (4 × 50 mL) and the separated organic layer was treated with distilled water (2 × 15 mL). The collected organic layer, after drying over anhydrous $MgSO_4$, was evaporated in vacuo to yield a white powder. *n*-Hexane (105 mL) was added dropwise to the dissolved white powder in acetone (15 mL) at ambient temperature for recrystallization. Then the recrystallized yield was collected by suction filtration in a Buchner funnel and dried under vacuum at room temperature. Yield: 5.06 g (81%). Mp: 51–53 °C. *Anal. Calcd.* for $C_{12}H_{18}O_4$ (226.12): C 63.70, H 8.02%; found: C 63.36, H 8.32%. FT-IR (KBr, cm^{-1}): 3400 (–OH), 3342 (H–O···H), 3080 (=CH aromatic), 2962, 2933, 2871 (–CH_2 aliphatic), 1593 (aromatic –C=C–), 1510, 1479, 1465, 1454, 1398, 1331, 1257 (Ar–O–CH_2), 1220, 1124, 1056 (Primary alcohol, C–O), 989, 956, 746. ^{1}H NMR ($CDCl_3$, δ, ppm): 6.86–6.82 (m, 4H, Ar*H*), 4.11 (t, J = 5.7 Hz, 4H, ArOCH_2), 3.80 (t, br, J = 5.0 Hz, 4H, $OCH_2CH_2CH_2OH$), 1.99 (p, J = 5.9 Hz, 4H, $OCH_2CH_2CH_2OH$), 1.68 (s, br, 2H, $OCH_2CH_2CH_2OH$). ^{13}C NMR ($CDCl_3$, δ, ppm): 148.34 (Ar*C*O), 121.32 (Ar*C*H), 112.97 (Ar*C*H), 67.80 (ArO*C*H_2), 61.13 (*C*H_2OH), 31.73 (OCH_2*C*H_2CH_2OH). MS (MICRO-MS, m/z): calcd. for $[M + Na + 2]^+$ 251.1259; found $[M + Na + 2]^+$ 251.2274.

3.3.2. *o*-Bis[3-(3,4-dicyanophenoxy)propyloxy]benzene (3)

o-Bis[(3-hydroxypropyl)oxy]benzene (**1**) (2.26 g, 0.01 mol) and 4-nitrophthalonitrile (**2**) (3.49 g, 0.02 mol) were mixed in 10 mL of dry DMF in a 100-mL reaction vessel and degassed 3 times with argon at room temperature. Finely pulverized K_2CO_3 (4.19 g, 0.03 mol) was added to the solution at 30-min intervals at 50 °C and stirred for 5 days while monitoring reaction progress by TLC (7:3 $CHCl_3$:PE) as a mobile phase. The cooled mixture was transferred into a 300-mL beaker containing 100 g of crushed ice and conc. HCl (5 mL) mixture and the obtained suspension was stirred for about 2–3 h. The precipitated green solid was filtered off and dried over P_2O_5 in a vacuum oven at 50 °C. Then the green product was recrystallized from MeOH (70 mL) at 50 °C for purification. The hot mixture was filtered to yield the purified **3** and then dried over P_2O_5 in a vacuum oven at 50 °C.

Yield: 2.96 g (62%). Mp: 115 °C. R_f: 0.50 (7:3 $CHCl_3$:PE). *Anal. Calcd.* for $C_{28}H_{22}N_4O_4 \cdot 0.5H_2O$ (487.17): C 68.97, H 4.76, N 11.50%; found; C 68.65, H 4.63, N 11.82%. FT-IR (KBr, cm^{-1}): 3114, 3074, 3043 (=CH aromatic), 2941, 2885 (–CH_2 aliphatic), 2227 (–C≡N), 1596 (aromatic –C=C–), 1564, 1506, 1473, 1406, 1334, 1323, 1255 (Ar-O-C), 1124, 1087, 1047, 840, 748. ^{1}H NMR (d_6-DMSO, δ, ppm): 7.98 (d, J = 8.5 Hz, 2H, Ar*H*), 7.70 (s, 2H, Ar*H*), 7.41 (d, J = 8.5 Hz, 2H, Ar*H*), 6.99 (s, br, 2H, Ar*H*), 6.88 (s, 2H, Ar*H*), 4.28 (t, br, J = 5.0 Hz, 4H, ArOCH_2), 4.10 (t, br, J = 5.0 Hz, 4H, $(NC)_2$ArOCH_2), 2.15 (p, br, J = 4.8 Hz, 4H, $OCH_2CH_2CH_2O$). ^{13}C NMR (d_6-DMSO, δ, ppm): 161.77 (C_4), 148.29 (C_{12}), 135.68 (C_6), 124.71 (C_{14}), 121.34 (C_5), 120.09 (C_3), 116.25–115.60 (C_7, C_8), 114.38 (C_{13}), 112.55 (C_2), 105.91 (C_1), 65.91 (C_{11}), 64.90 (C_9), 28.29 (C_{10}). MS (ESI-MS) m/z = 479.3, 501.2, 517.1 calcd. for $[M + 1]^+$, $[M + Na]^+$, $[M + K]^+$.

3.4. Polymer synthesis

3.4.1. Synthesis of polymeric metal-free phthalocyanine (4)

A mixture of (0.479 g, 1.0 mmol) **3** and 4.0 mL of dry amyl alcohol was stirred in a standard Schlenk tube and degassed. After the reaction temperature was raised to 90 °C, 1,8-diazabicyclo[5.4.0]undec-7-ene (DBU) (0.15

mL, 0.16 g, 1.0 mmol) was added to the Schlenk tube, followed by further degassing. The reaction mixture was heated to 160 °C and stirred for 24 h. The cooled residue in the Schlenk tube was transferred into a flask with EtOH at room temperature. The solvent was removed under vacuum using evaporator. The precipitated product was triturated with 30 mL of EtOH/distilled H_2O (1:1 v/v). After being filtered by vacuum filtration using a sintered glass funnel, the raw product was treated with EtOH/H_2O mixture, Et_2O, and acetone, consecutively. The pure dark green product was dried under vacuum until dryness.

Yield: 0.39 g (81%). Mp: 330 °C. *Anal. Calcd.* for $(C_{112}H_{90}N_{16}O_{16})_n$ (1914.67) (for C≡N end groups): C, 70.21; H, 4.73; N, 11.70%; found: C, 69.86; H, 5.15; N, 12.13%. FT-IR (KBr, cm^{-1}): 3285 (N–H), 3093, 3032 (=CH aromatic), 2921, 2855 (–CH_2 aliphatic), 2224 (–C≡N), 1645 (–C=N–), 1614 (aromatic –C=C–), 1558, 1506, 1489, 1456, 1339, 1225 (Ar–O–C), 1114, 1091, 1045 (N–H), 821, 742.

3.4.2. Synthesis of polymeric zinc phthalocyanine (5)

To a 25-mL reaction flask (0.479 g, 1.0 mmol) **3**, 5.0 mL of dry amyl alcohol and $Zn(CH_3COO)_2$ (0.184 g, 1.0 mmol) were loaded and degassed twice. DBU (0.15 mL, 0.16 g, 1.0 mmol) was slowly added to the reaction flask after heating to 90 °C. The reaction mixture was stirred at 160 °C for 24 h. After cooling, a minimal amount of Et_2O was added to the flask, followed by mixing for 45 min. The precipitation was filtered off using a sintered glass Buchner funnel and purified with washing with EtOH/pure H_2O (1:1 v/v), EtOH, H_2O, *n*-hexane, and Et_2O. The final dark green solid (**5**) was dried under vacuum until dryness.

Yield: 0.46 g (90%). Mp: > 300 °C. *Anal. Calcd.* for $(C_{112}H_{92}N_{12}O_{24}Zn)_n$ (2052.56) (for imide end groups): C, 65.45; H, 4.51; N, 8.18; Zn, 3.18%; found: C, 65.83; H, 4.90; N, 8.01; Zn, 2.94%. FT-IR (KBr, cm^{-1}): 3331 (imide N–H), 3062 (=CH aromatic), 2931, 2875 (–CH_2 aliphatic), 1769 (sym. C=O), 1713 (asym. C=O), 1647 (–C=N–), 1597 (aromatic –C=C–), 1489, 1467, 1253, 1224 (Ar–O–C), 1120–1045, 964, 833, 759, 746.

3.4.3. Synthesis of polymeric nickel and copper phthalocyanines (6, 7)

To a 25-mL reaction flask (0.479 g, 1.0 mmol) **3**, 5.0 mL of dry DMEA, and anhydrous $NiCl_2$ (0.150 g, 1.0 mmol) or anhydrous $CuCl_2$ (0.135 g, 1.0 mmol) were loaded and degassed 3 times. Next the temperature of the reaction medium was raised to 90 °C and

DBU (0.15 mL, 0.16 g, 1.0 mmol) was slowly added dropwise to the reaction vessel. The reaction was continued with stirring at 170 °C for 24 h. The cooled reaction content was transferred into a flask with EtOH. The solvent mixture was evaporated by a rotary evaporator under reduced pressure to give green products. Afterwards, the crude green products were suspended with EtOH/distilled H_2O (1:1 v/v), filtered off, and purified by washing with MeOH, $CHCl_3$, DMF, H_2O, and Et_2O, consecutively. Final green (**6**) and dark green (**7**) products were dried under vacuum until dryness.

Compound **6**

Yield: 0.43 g (84%). Mp: > 300 °C. *Anal. Calcd.* for $(C_{112}H_{92}N_{12}O_{24}Ni)_n$ (2046.57) (for imide end groups): C, 65.66; H, 4.53; N, 8.20; Ni, 2.86%; found: C, 65.26; H, 4.79; N, 7.76; Ni, 3.18%. FT-IR (KBr, cm^{-1}): 3398 (imide N–H), 3065 (=CH aromatic), 2951, 2910, 2864 (–CH_2 aliphatic), 1771 (sym. C=O), 1715 (asym. C=O), 1651 (–C=N–), 1593 (aromatic –C=C–), 1463, 1229 (Ar–O–C), 1120–1045, 823, 740, 549.

Compound **7**

Yield: 0.45 g (∼88%). M.: > 300 °C. *Anal. Calcd.* for $(C_{112}H_{92}N_{12}O_{24}Cu)_n$ (2051.56) (for imide

end groups): C, 65.51; H, 4.52; N, 8.18; Cu, 3.09%; found: C, 65.12; H, 4.27; N, 8.60; Cu, 3.47%. FT-IR (KBr, cm^{-1}): 3410 (imide N–H), 3132, 3046 (=CH aromatic), 2949, 2869 (–CH_2 aliphatic), 1767 (sym. C=O), 1705 (asym. C=O), 1647 (–C=N–), 1608 (aromatic –C=C–), 1587, 1472, 1385, 1236 (Ar–O–C), 1122–1054, 954, 836, 732, 514.

3.4.4. Synthesis of polymeric cobalt phthalocyanine (8)

A 25-mL reaction flask was charged with (0.479 g, 1.0 mmol) **3**, 5.0 mL of dry ethylene glycol, and anhydrous $CoCl_2$ (0.130 g, 1.0 mmol) and degassed by argon several times; then 40 mg of ammonium molybdate as a catalyst was added. After the reaction suspension was refluxed at 220 °C with stirring under argon for 24 h, 10 mL of EtOH was slowly added to the cooled reaction flask, followed by stirring for 30 min. The solvent was removed under vacuum and EtOH/distilled H_2O (1:1 v/v) was poured onto the resulting green product. To obtain pure product, the precipitated green product was filtered and treated with EtOH/distilled H_2O (1:1 v/v), MeOH, DMF, PE, H_2O, and Et_2O. The desired product was dried under vacuum until dryness.

Yield: 0. 43 g (84% when catalyst used) and 0.21 g (49% when catalyst not used). Mp: > 300 °C. *Anal. Calcd.* for $(C_{112}H_{92}N_{12}O_{24}Co)_n$ (2047.56) (for imide end groups): C, 65.65; H, 4.53; N, 8.20; Co, 2.88%; found: C, 65.93; H, 4.69; N, 8.52; Co, 3.14%. FT-IR (KBr, cm^{-1}): 3396 (imide N–H), 3037, 3016, 3007 (=CH aromatic), 2957, 2936, 2876 (–CH_2 aliphatic), 1771 (sym. C=O), 1716 (asym. C=O), 1650 (–C=N–), 1606 (aromatic –C=C–), 1542, 1496, 1488, 1387, 1232 (Ar–O–C), 1120–1047, 964, 827, 744, 642.

3.5. The conversion of cyano end groups of the polymeric metal-free phthalocyanine into imido groups (4a)

The conversion of cyano end groups of the polymeric metal-free phthalocyanine into imido groups was performed according to the literature with small changes in the purification part.[20,28,30] The polymeric metal-free phthalocyanine with imido end groups was dried under vacuum after the appropriate purification steps.

Yield: 0.19 g (∼90%). Mp: > 300 °C. *Anal. Calcd.* for $(C_{112}H_{94}N_{12}O_{24})_n$ (1990.65) (for imide end groups): C, 67.53; H, 4.76; N, 8.44%; found: C, 67.78; H, 4.37; N, 8.69%. FT-IR (KBr, cm^{-1}): 3396 (imide N–H), 3278 (N–H), 3068, 3042 (=CH aromatic), 2970, 2945, 2840 (–CH_2 aliphatic), 1770 (sym. C=O), 1716 (asym. C=O), 1652 (–C=N–), 1610 (aromatic –C=C–), 1560, 1519, 1506, 1480, 1421, 1337, 1236, 1227 (Ar–O–C), 1166, 1113, 1090, 1040 (N–H), 995, 959, 824, 735, 632.

Acknowledgments

Financial support from Kocaeli University Scientific Research Projects Unit (Project number BAP-2010/38) is acknowledged. We wish to thank Assoc Prof Dr Muhammet Işıklan (Kırıkkale University) for his assistance with the elemental analysis, and DSC and TGA measurements.

References

1. Moser, F. H.; Thomas, A. L. *The Phthalocyanines;* Vols I–II; CRC Press Inc.: Boca Raton, FL, USA, 1983.
2. Leznoff, C. C.; Lever, A. B. P., Eds. *Phthalocyanines: Properties and Applications;* Vols. 1–4, VCH Publishers (LSK) Ltd.: Cambridge, UK, 1989, 1993, 1993, 1996.
3. Wöhrle, D.; Schulte, B. *Macromol. Chem.* **1985**, *186*, 2229–2245.

4. Özçelik, S.; Karaoğlan, G. K.; Gümrükcü, G.; Gül, A. *Turk. J. Chem.* **2012**, *36*, 899–906.
5. Achar, B. N.; Fohlen, G. M.; Parker, J. A. *J. Appl. Polym. Sci.* **1984**, *29*, 353–359.
6. Wright, J. D.; Roisin, P.; Rigby, G. P.; Nolte, R. J. M.; Cook, M. J.; Thorpe, S. C. *Sensors & Actuators B* **1983**, *13*, 276–280.
7. Radhakrishnan, S.; Deshpande, S. D. *Sensors* **2002**, *2*, 185–194.
8. Boyle, R. W.; Leznoff, C. C.; van Lier, J. E. *Br. J. Cancer.* **1993**, *67*, 1177–1181.
9. Gregory, P. *J. Porphyrins Phthalocynines* **2000**, *4*, 432–437.
10. Inabe, T.; Tajima, H. *Chem. Rev.* **2004**, *104*, 5503–5534.
11. Wung, J.; Pamidi, P. V. A; Purrado, C.; Park, D. S.; Pingarron, J. *Electroanalysis* **1997**, *9*, 908–911.
12. Rohlfing, D. F.; Rathouský, J.; Rohlfing, Y.; Bartels, O.; Wark, M. *Langmuir* **2005**, *21*, 11320–11329.
13. Yamaki, J.; Yamaji, A. *J. Electrochem. Soc.* **1982**, *129*, 5–9.
14. Rieke, P. C.; Armstrong, N. R. *J. Am. Chem. Soc.* **1984**, *106*, 47–50.
15. Ün, İ.; Zorlu, Y.; İbişoğlu, H.; Dumoulin, F.; Ahsen, V. *Turk. J. Chem.* **2013**, *37*, 394–404.
16. Ogbodu, R. O.; Nyokong, T. *J. Photochem. Photobiol. A* **2014**, *274*, 83–90.
17. Büchel, K. H.; Falbe, J.; Hagemann, H; Hanack, M.; Klamann, D.; Kreher, R.; Kropf, H.; Regitz, M.; Schaumann, E., Eds. Houben-Weyl – *Methods of Organic Chemistry, Additional and Supplementary* Volumes of the 4th edn, Vol. E9, Georg Thieme Verlag: Stuttgart, Germany, 1998, pp. 717–843.
18. Wöhrle, D. *Macromol. Rapid. Commun.* **2001**, *22*, 68–97.
19. Kimura, M.; Nishigaki, T.; Koyama, T.; Hanabusa, K.; Shirai, H. *Macromol. Chem. Phys.* **1994**, *195*, 3499–3594.
20. Bilgin, A.; Yağcı, Ç.; Yıldız, U. *Macromol. Chem. Phys.* **2005**, *206*, 2257–2268.
21. Hanack, M.; Datz, A.; Fay, R.; Fischer, K.; Keppeler, U.; Koch, J.; Metz, J.; Metzger, M.; Schneider, O.; Schulze, H. In *Handbook of Conducting Polymers*, Skotheim, TA, Ed. Marcel Dekker: New York, NY, USA, 1986, pp. 133–204.
22. Venkatachalam, S.; Rao, K. V. C.; Manoharan, P. T. *J. Polym. Sci., Part B: Polym. Phys.* **1994**, *32*, 37–52.
23. Achar, B. N.; Fohlen, G. M.; Parker, J. A. *J. Polym. Sci., Polym. Chem. Ed.* **1982**, *20*, 1785–1790.
24. Wöhrle, D.; Hüdorf, U. *Makromol. Chem.* **1985**, *186*, 2177–2187.
25. Budd, P. M.; Makhseed, S. M.; Ghanem, B. S.; Msayib, K. J.; Tattershall, C. E.; McKeown, N. B. *Materials Today* **2004**, *7*, 40–46.
26. Yağcı, Ç.; Bilgin, A. *J. Porphyrins Phthalocyanines* **2013**, *17*, 573–586.
27. Yağcı, Ç.; Bilgin, A. *Polyhedron* **2013**, *51*, 142–155.
28. Bilgin, A.; Yağcı, Ç.; Yıldız, U; Özkazanç, E.; Tarcan, E. *Polyhedron* **2009**, *28*, 2268–2276.
29. Bilgin, A.; Mendi, A.; Yıldız, U. *Polymer* **2006**, *47*, 8462–8473.
30. Bilgin, A.; Yağcı, Ç.; Mendi, A.; Yıldız, U. *J. Appl. Polym. Sci.* **2008**, *110*, 2115–2126.
31. Ahsen, V.; Yılmazer, E.; Bekâroğlu, Ö. *Makromol. Chem.* **1988**, *189*, 2533–2543.
32. Kyba, E. P.; Davis, R. E.; Hudson, C. W.; John, A. M.; Brown, S. B.; McPhaul, M. J.; Liu, L. K.; Glover, C. *J. Am. Chem. Soc.* **1981**, *103*, 3868–3875.
33. Chen, C. S.; Wang S. J.; Wu, S. C. *Org. Prep. Proced. Int.* **1982**, *14*, 350–353.
34. Young, G. J.; Onyebuagu, W. *J. Org. Chem.* **1990**, *55*, 2155–2159.
35. Brewise, M.; Clarkson, G. J.; Helliwell, M.; Holder, A. M.; McKeown, N. B. *Chem. Eur. J.* **2000**, *6*, 4630–4636.
36. Nemykina, V. N.; Luk'yanets, E. A. *Arkivoc* **2010**, *i*, 136–208.
37. Sidorov, A. N.; Kotylar, I. P. *Opt. Spectrosc.* **1961**, *11*, 92–96.
38. Snow, A. W.; Griffith, J. R.; Marullo, N. P. *Macromolecules* **1984**, *17*, 1614–1624.

39. Wöhrle, D.; Marose, U.; Knoop, R. *Makromol. Chem.* **1985**, *186*, 2209–2228.
40. Wöhrle, D.; Preußner, E. *Makromol. Chem.* **1985**, *186*, 2189–2207.
41. Nakomato, K. *Infrared Spectra of Inorganic and Coordination Compounds*, 2nd edn, Wiley: New York, NY, USA, 1970.
42. Wöhrle, D.; Benters, R.; Suvorova, O.; Schnurpfeil, G.; Trombach, N.; Bogdahn-Rai, T. *J. Porphyrins Phthalocyanines* **2000**, *4*, 491–497.
43. Kabay, N.; Gök, Y. *Tetrahedron. Lett.* **2013**, *54*, 4086–4090.
44. Gök, Y.; Kantekin, H.; Bilgin, A.; Mendil, D.; Değirmencioğlu, İ. *J. Chem. Soc., Chem. Commun.* **2001**, *3*, 285–286.
45. Cuellar, E. A.; Marks, T. J. *Inorg. Chem.* **1981**, *20*, 3766–3770.
46. Kobayashi, N.; Furuyama, T.; Satoh, K. *J. Am. Chem.* **2011**, *133*, 19642–19645.
47. Atilla, D.; Aslıbay, G.; Gürek, A. G.; Can, H.; Ahsen, V. *Polyhedron* **2000**, *26*, 1061–1069.
48. Sielcken, O. E.; Tilborg, M. M. V.; Roks, M. F. M., Hendriks, R.; Drenth, W.; Nolte, R. J. M. *J. Am. Chem. Soc.* **1987**, *109*, 4261–4265.
49. Snow, A. In *The Porphyrin Handbook: Properties and Materials*, Kadish, K. M.; Smith, K. M.; Guilard, R., Eds. Vol. 17, Elsevier Science: Amsterdam, Holland, 2003, pp. 129–176.
50. Özceşmeci, İ.; Gelir, A.; Gül, A. *Dyes Pigments* **2012**, *92*, 954–960.
51. Choi, M. T. M.; Li, P. P. S.; Ng, D. P. K. *Tetrahedron* **2000**, *56*, 3881–3887.
52. Ledson, D. L.; Twigg, M. V. *Chem. Ind.* **1975**, *3*, 129–130.
53. George, D. R.; Snow, A. W.; Shirk, J. S.; Barger, W. R. *J. Porphyrins Phthalocyanines* **1998**, *2*, 1–7.
54. Lopez, T.; Ortiz, E.; Alvarez, M.; Navarrete, J.; Odriozola, J. A.; Ortega, F. M.; Páez-Mozo, E. A.; Escobar, P.; Espinoza, K. A.; Rivero, I. A. *Nanotech. Biol. Med.* **2010**, *6*, 777–785.
55. Sielcken, O. E.; Nolte, R. J. M; Schoonman. *J. Reacl. Trav. Chim. Pays-Bas* **1990**, *109*, 230–234.
56. Liao, M. S.; Kuo, K. *J. Polym. Sci. A* **1990**, *28*, 2349–2357.
57. Achar, B. N.; Fohlen, G. M.; Parker, J. A.; Keshavayya, J. *J. Polym. Sci., Polym. Chem. Ed.* **1987**, *25*, 443–450.
58. Lever, A. B. P. *Adv. Inorg. Chem. Radiochem.* **1965**, *7*, 27–114.
59. Odabaş, Z.; Orman, E. B.; Durmuş, M.; Dumludağ, F.; Özkaya, A. R.; Bulut, M. *Dyes Pigments* **2012**, *95*, 540–552.
60. Savaran, S.; Mathai, C. S.; Anantharaman, M. R.; Venkatachalam, S.; Prabhakaran, P. V. *Appl. Polym. Sci.* **2004**, *91*, 2529–2535.
61. Vijayakumar, P. S.; Pohl, H. *J. Polym. Sci. Polym. Phys.* **1984**, *22*, 1439–1452.
62. Arii, T.; Kishi, A. *Thermochim. Acta* **2003**, *400*, 175–185.
63. Charles, J. N.; Desphande, N. D.; Desphande, D. A. *Thermochim. Acta* **2001**, *375*, 169–176.
64. Schmitt, M.; Janson, O.; Schmidt, M.; Hoffmann, S.; Schnelle, W.; Drechsler, S. L.; Rosner, H. *Phys. Rev. B* **2009**, *79*, 245119.
65. Ribas, J.; Escuer, A.; Serra, M.; Vicente, R. *Thermochim. Acta* **1986**, *102*, 125–135.
66. Desphande, D. A.; Ghormare, K. R.; Desphande, N. D.; Tankhiwale, A. V. *Thermochim. Acta* **1993**, *66*, 255–265.
67. Perin, D. D.; Armarego, W. L. F. *Purification of Laboratory Chemicals*, 2nd edn, Pergamon Press: Oxford, UK, 1989.